ARCHIVES OF ACOUSTICS
26, 3, 223–233 (2001)

NUMERICAL AND EXPERIMENTAL PRESSURE DETERMINATION IN THE VERY NEAR FIELD OF A PIEZOELECTRIC TRANSDUCER

L. FILIPCZYŃSKI, T. KUJAWSKA, J. WÓJCIK

and T. TYMKIEWICZ

Polish Academy of Sciences
Institute of Fundamental Technological Research
(00-049 Warszawa, Świętokrzyska 21, Poland)

Measurements in the very near field of piezoelectric transducers are fundamental for many ultrasonic problems. In such cases also the transducer vibrations should be known to perform mathematical models of radiated beams. Acoustic pressure measurements near to the transducer surface can give the necessary information. The pressure of the radiated wave at the transducer surface corresponds to its normal vibration velocity multiplied by the ρc value of the medium. However, this is valid only for the central wave, when the edge wave of the transducer can be ignored. On the other hand, pressure measurements on and very near to the transducer surface are not possible because of the voltage leakage between the electronic transmitter and the PVDF hydrophone used in such measurements. By means of a numerical model, central and edge waves were found for a plane PZT transducer 7.5 mm in radius, with the applied 2.7 MHz voltage pulse composed of 3 cycles. Two types of boundary conditions of Dirichlet and Neumann were considered showing a negligible difference in the case of short pulses. Basing on numerical and experimental results, practical conditions were determined which make it possible to carry out pressure measurements in the very near field of the transducer, and hence to determine the transducer vibrations which are important for modeling ultrasonic pulse beams.

1. Introduction

In many ultrasonic applications the knowledge of transducer vibrations and their surface distribution is decisive for modeling the radiated ultrasonic beams. Hence the experimental results obtained in ultrasonic devices can be compared with the theoretical ones showing possible optimal solutions predicted by the theory. One of the methods used for determination of transducer vibrations is the measurement of the wave pressure in the liquid medium, near to the transducer surface, by means of the wide band piezoelectric polymer hydrophone PVDF. However, the structure of the near field is very complex due to the interaction of central and edge waves in this region. On the other hand, pressure measurements on and very near to the transducer surface are not possible because of the voltage leakage between the electronic transmitter and the PVDF hydrophone used

in measurements. The purpose of the present paper is to investigate and to establish necessary conditions in the very near field which make it possible to determine vibrations of the transducer surface by means of pressure measurements.

2. Central and edge waves

Complex structure of the near field is caused by the interference of the central wave which is radiated by the front surface of the transducer and of the edge wave generated by the transducer contour. This problem was extensively discussed by HUTCHINS and HAYWARD [4] and confirmed experimentally by many authors in the case of plane and concave transducers (see for example [1]). The generation of edge waves can by easily explained by means of the Fresnel zones (see Appendix).

The pressure on the transducer plane surface $p(z=0,t)$ corresponds exactly to the normal acoustic velocity $v(t)$ according to the relation

$$p(z=0,t) = \rho c \cdot v(t). \tag{1}$$

In the case when the edge wave interferes with the central wave, the relation (1) is no more valid [5]. Relation (1) is practically fulfilled on the axis of the circular transducer near to its surface. Outside of the axis it can be fulfilled only in such a case when the contribution of the edge wave is so small in relation to the central wave that it can be neglected.

3. Parameters of the examined system and the experimental equipment

The considered system was composed of an electronic pulse transmitter with the carrier frequency of 2.7 MHz. The generated ultrasonic pulses composed of 3 cycles and their spectrum are shown in Fig. 1. The voltage applied to the transducer was equal to $40V_{\mathrm{pp}}$. The radius of the circular plane PZT transducer equaled 7.5 mm. Pressure measurements were performed in a water container by means of the PVDF bilaminar membrane hydrophone, model 800 (Sonic Technologies), calibrated by the National Physical Laboratory (Teddington, England) with the sensitive electrode diameter of 0.6 mm. Since PZT transducers in such conditions are linear devices [2], the whole measurement system can be considered also as a linear one for small distances z from the transducer. For distances up to $z = 40$ mm we did not observe any nonlinear effects. They may be expected for higher values of z being caused by nonlinear propagation in water. Since we examine the medium near to the transducer, the system can be considered as linear.

The velocity distribution on the transducer surface was assumed to be uniform for the radius $r < 7.5$ mm and zero for $r > 7.5$ mm. In reality, the uniform distribution of amplitudes and phases can be considered as a rather good approximation when the back side of the transducer is acoustically heavily loaded [6].

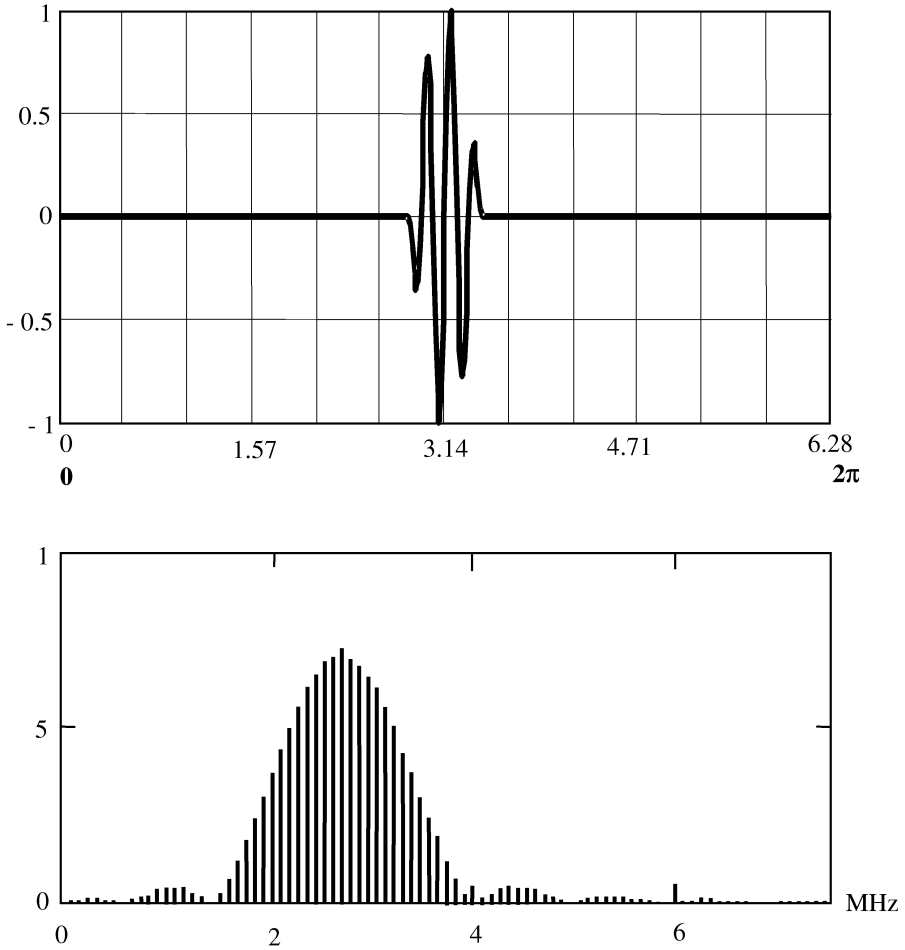

Fig. 1. The shape of the ultrasonic pulse assumed for computations (top) and its spectrum (bottom).

4. The numerical procedure

Two types of boundary problems were solved numerically: the Dirichlet and Neumann ones [8]. Dirichlet conditions fix the value of the scalar acoustic potential ϕ related directly to the acoustic pressure by the relation $p = (-)\rho\,\partial\phi/\partial t$. Neumann conditions fix its gradient $\partial\phi/\partial n$ which is equal to the acoustic velocity $(+) - v$. The signs of pressure and velocity shown in brackets are used in mechanics while the other ones outside the brackets are employed in acoustics [7].

The D'Alembert solution of the wave equation for the half-space $z \geq 0$ with the plane boundary $S(x, y, z = 0)$ can be expressed in the form

$$P(\mathbf{x}, \tau) = \frac{1}{2}\sum_{i=1} P_n(\mathbf{x}) e^{-in\tau} + c.c, \qquad P_n = i \cdot n \cdot \phi_n\,, \tag{2}$$

where $\mathbf{x} \equiv (x, y, z)$, $\mathbf{x} = k_0 \mathbf{x}_w$, $t = \omega_0 t_w$ – dimensionless coordinates; $\mathbf{x}_w$, t_w – dimensional coordinates, *c.c.* – conjugate quantity, $\tau = t - z/c_0$ – retarded dimensionless time, $k_0 c_0 = \omega_0$, $n = \omega_n/\omega_0$ – dimensionless pulsation, $\{P_n\}$, $\{\phi_n\}$ – Fourier spectra of the pressure and of the acoustic potential, $\phi_n(\mathbf{x})$ – Rayleigh-Sommerfeld solutions of the Dirichlet problem

$$\phi_n(\mathbf{x}) = e^{-inz} \int_S \phi_n(S') \frac{\partial G(\mathbf{x}, S')}{\partial s'} dS', \qquad \frac{\partial G^-(\mathbf{x}, S')}{\partial s'} \equiv \frac{1}{2\pi} \frac{z}{R} \frac{\partial}{\partial R} \frac{e^{inR}}{R} \tag{3}$$

and of the Neumann problem

$$\phi_n(\mathbf{x}) = -e^{-inz} \int_S v_{n,s'} G(\mathbf{x}, S') dS', \qquad G^+(\mathbf{x}, S') \equiv \frac{1}{2\pi} \frac{e^{inR}}{R}, \tag{4}$$

where $R \equiv \sqrt{(x - x')^2 + (y - y')^2 + z^2}$; $v_{n,s'} \equiv (\partial/\partial s')\phi_n$ – component of the velocity vector normal to the surface $S(\mathbf{x})$, $S(x = x', y = y', z = z' = 0) = S'$; s' – unit vector normal to S; G^+, G^- – Green functions [9, 11]. $\phi_n(\mathbf{x})$ – fulfils the Helmholtz equation $\Delta\phi_n + n^2\phi = 0$.

The numerical algorithm for the pressure determination in the ultrasonic beam radiated by the piezoelectric transducer excited by the short pulse was determined from Eqs. (3) and (4) by means of the spectral analysis. Calculations were performed for two boundary conditions. In the first, the Dirichlet case, the constant pressure on the transducer surface and zero pressure outside of it was assumed. In the second, the Neumann case, the transducer was mounted in a infinitely rigid baffle and its acoustic velocity in the direction of z was constant on the transducer surface and zero outside of it.

In both cases, the dimensionless system of variables in time and frequency was applied. The carrier frequency of the radiated pulse with the normalized amplitude corresponded to the frequency of the main spectral line f_m. The normalization base of λ_0 determined the sampling scale in time and in frequency for the known propagation velocity c_0 in the medium. The normalization base was chosen to equate the repetition time of the radiated frequency $1/f_0$ with the dimensionless time 2π, where $f_0 = c_0/\lambda_0$ denotes the sampling frequency of the spectrum. Then the fundamental lobe of the spectrum contains the number of spectral lines equal to $N_m = f_m/f_0$. The amplitude of every spectral line depends also on the radiated pressure pulse wave-form. The envelope of the simulated pulse was chosen analytically to fit maximally the real pressure wave-form.

The next step of numerical calculations was the determination of pressure in an arbitrary point of the radiated ultrasonic beam for the transducer excited by the unit amplitude continuous wave with various frequencies corresponding to the frequency nf_0 of the n-th spectral line of the pulse. For this purpose the method of the surface integral based on the Huygens principle was applied. Multiplying spectra for the same spatial point and applying the inverse Fourier transform, the spatial distribution of the pressure field of the ultrasonic transducer excited by short pulses was determined.

Figure 2 presents pressure amplitude distributions along the beam axis computed numerically for Dirichlet boundary conditions of the transducer. It means that the acoustic

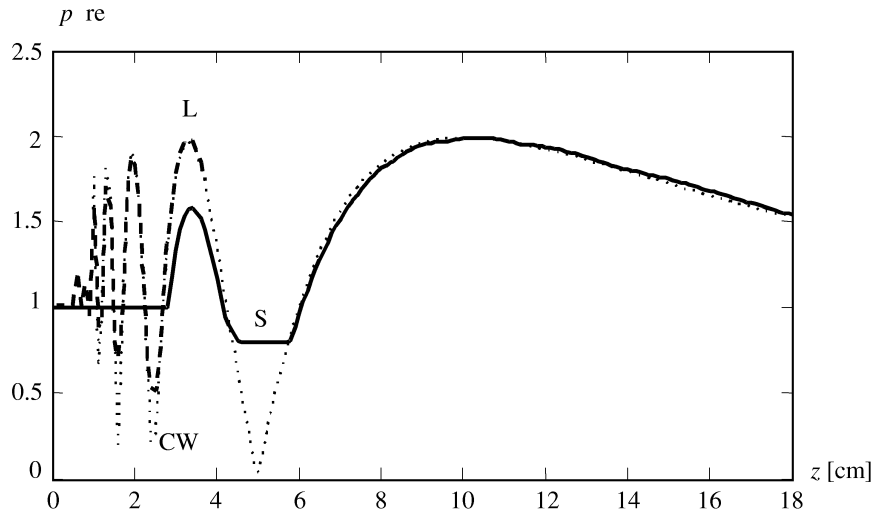

Fig. 2. Amplitude pressure distributions computed along the transducer beam axis z in the case of Dirichlet boundary conditions. CW (dotted line) denotes continuous waves, L (dashed line) – long and S (full line) – short pulses (see Fig. 3).

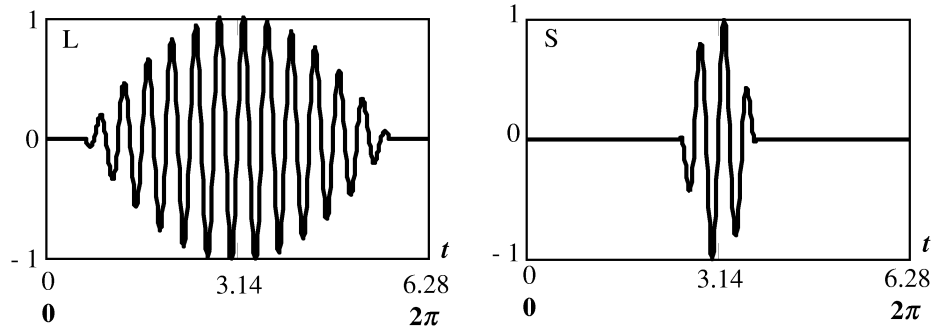

Fig. 3. The shapes of the long (L) and short (S) pulses assumed for computations.

pressure is assumed to be constant on the transducer surface and zero outside of it (at the plane $z = 0$). The computations were performed for continuous waves, for long and for short pulses. Figure 3 shows the shapes of pulses used in computations.

Similar computations were carried out for Neumann boundary conditions as shown in Fig. 4 where the normal component of the acoustic velocity is constant over the transducer face and is zero outside it. The pressure distribution in the case of continuous waves can be found analytically showing a series of maxima of constant amplitude with intervening nulls. In the case of our calculations the density of the points determined numerically was too low to follow the details of this series.

However, in real probes used in ultrasonography the Neumann boundary conditions are suitable. If the transducer could be considered as a liquid surface or freely suspended in a fluid with no other buffle being present, then the Dirichlet boundary condition would

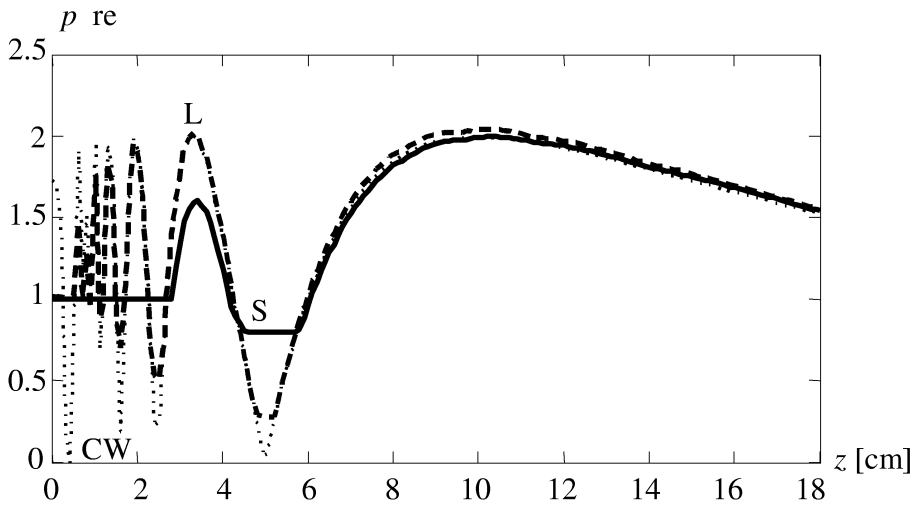

Fig. 4. Amplitude pressure distributions computed along the transducer beam axis z in the case of Neumann boundary conditions. All notations as in Fig. 2.

be adequate [4]. Therefore our considerations concern mainly the Neumann boundary condition corresponding to the construction of real ultrasonic transducers used for example in ultrasonography.

5. Discussion and conclusions

Measurements of the acoustic pressure in the very near field of the piezoelectric transducer make it possible to obtain information on the acoustic velocity of the vibrating transducer. However, this is possible when the edge wave interfering with the central wave can be neglected. Figure 5 shows the computed central and edge waves and their interference along the transducer axis when increasing the distance z. The pressure amplitudes of the central and edge waves are the same, however their phases are reversed (see Fig. 5 top).

Using the described numerical procedure, the influence of the distance from the transducer on the amplitude of the edge wave could be shown. So the minimum distance from the transducer can be found for which it is possible to determine the amplitude of the acoustic velocity on the transducer surface by means of pressure measurements, without introducing significant errors. In our case this distance determined numerically and experimentally was equal to $z = 4\,\mathrm{mm}$ (Fig. 6). In such a case, the pressure amplitude on the transducer edge is only by about 10% $\Leftrightarrow$ 1 dB higher than the amplitude of the central part of the transducer forming there the central wave. However, when increasing the distance z to 10 and 36 mm, the influence of the edge wave becomes very high (Figs. 7 and 8). Then conclusions regarding the transducer vibrations from pressure measurements would be wrong.

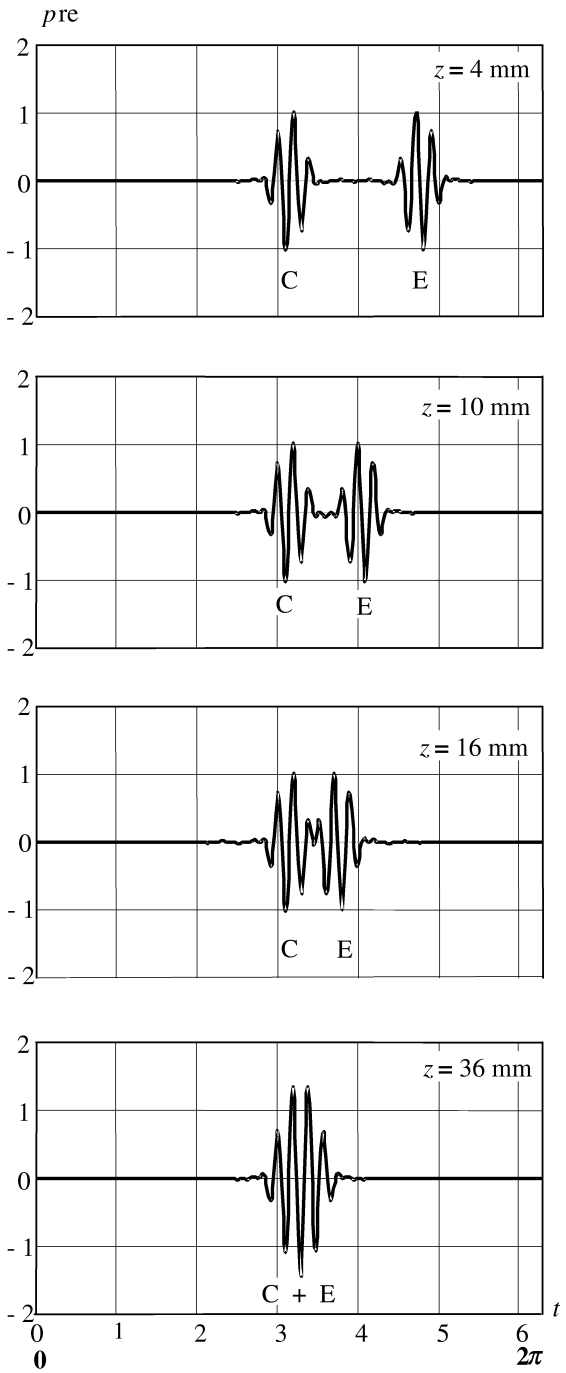

Fig. 5. Interference of the computed central wave C with the edge wave E at the transducer beam axis for various distances $z = 4$, 10, 16 and 36 mm. The computations were performed for the Neumann boundary condition.

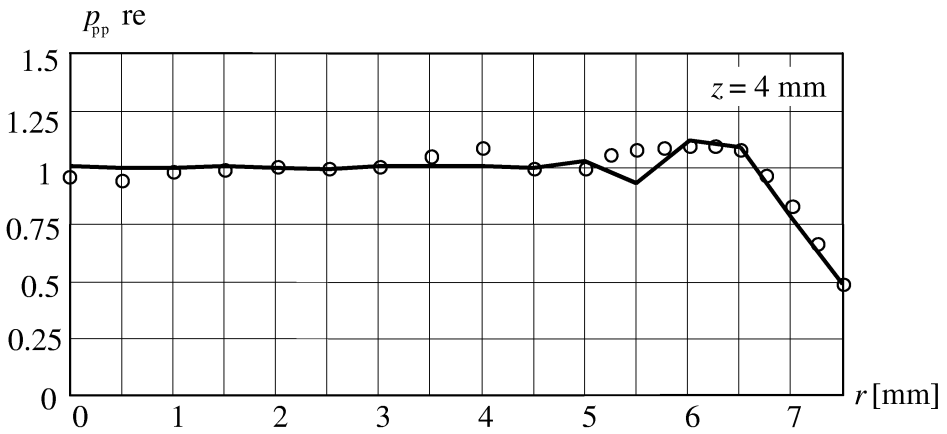

Fig. 6. The computed (solid line) and measured (points) pressure distributions before the face of the transducer at the distance of $z = 4$ mm. The radial distance from the transducer symmetry axis is denoted by r.

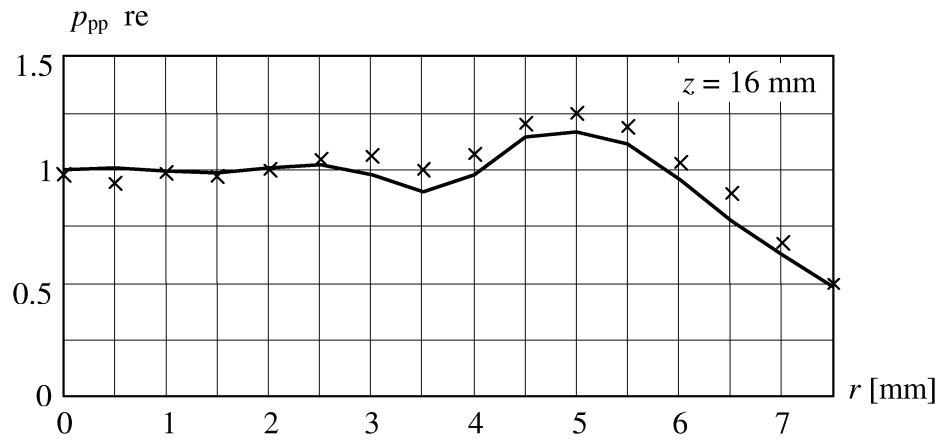

Fig. 7. As in Fig. 6, however at the distance of $z = 16$ mm.

In a similar way also the minimum distance on the transducer beam axis can be found where the acoustic velocity of the transducer can be determined by means of pressure measurements. This distance is now much greater; in the case under consideration it is equal to $z = 20$ mm as shown in Fig. 9.

In this way one can obtain by means of pressure measurements, the information on transducer vibrations which is important for modeling the ultrasonic pulse beams used in various applications.

It is interesting to notice that for the Dirichlet and Neumann boundary conditions, pressure distributions in the near field differ significantly. However, this difference is much smaller for long pulses and disappears for short pulses as shown in Figs. 2 and 4.

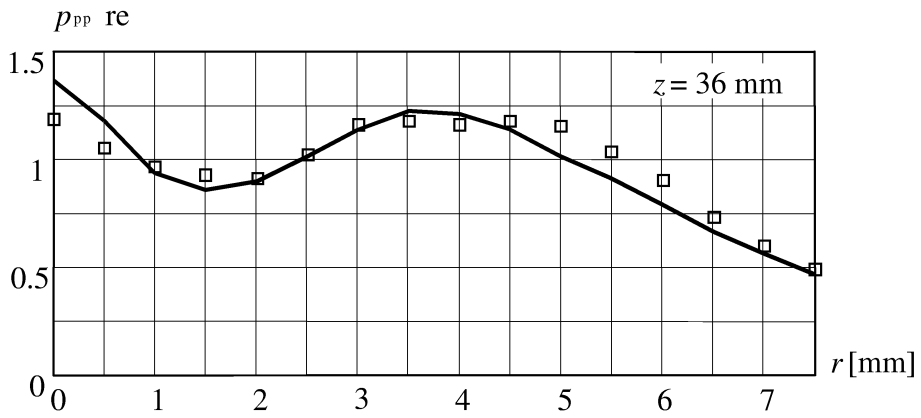

Fig. 8. As in Fig. 6, however at the distance of $z = 36$ mm.

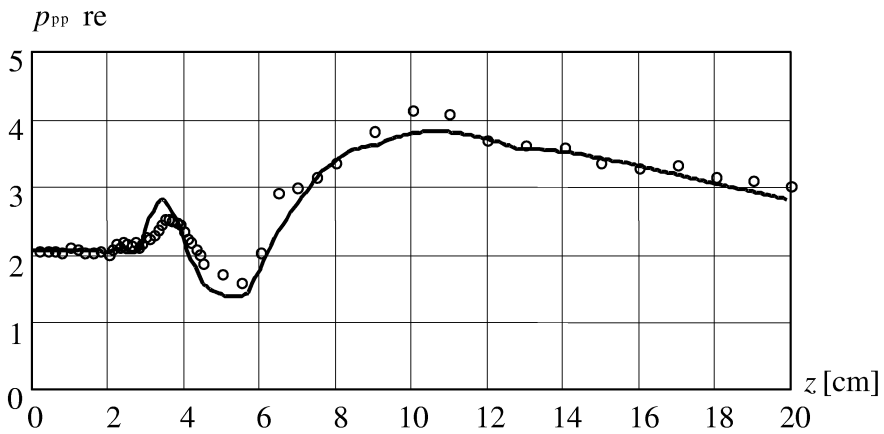

Fig. 9. The computed (solid line) and measured (points) pressure distributions along the transducer beam axis z.

Appendix. Interpretation of edge waves by means of Fresnel zones

Consider a vibrating circular plane surface which is divided into a number of concentric Fresnel zones. The slant distance from the observation point P is greater by $\lambda/2$ than that of the neighbour zone of the smaller diameter. It can be shown [10] that the area of the n zone is given by $\pi \mathbf{x} \lambda$ if λ is small compared with the distance x of the point P from the transducer (see Fig. 7.6 in [10]). The surface of every zone is the same and equal to the surface of the first zone $S = \pi \mathbf{x} \lambda$.

The amplitude of waves radiated by every zone is an arithmetic mean between both the neighbouring waves, independently of how may they decrease [3]. Let us denote the contribution of the n zone by z_n. Then the contribution of all zones at the point P equals (see Fig. 825 in [3]).

$z = z_1 - z_2 + z_3 - z_4 + z_5 - \ldots$ or $z = z_1/2 + (z_1/2 - z_2 + z_3/2) + (z_3/2 - z_4 + z_5/2) + \ldots$

Because all the values in parentheses equal zero, we obtain finally

$$z = z_1/2. \tag{A1}$$

Hence it follows that the contribution of all the radiated waves in their full extent, embracing all the Fresnel zones, is equivalent to the contribution of half of the first Fresnel zone.

In the case of a circular transducer with radius r, a similar construction of Fresnel zones can be performed, however now for the plane outside of the transducer (for greater radii than r). So the distance of the Fresnel zones from the point P equals now $b + \lambda/2$, $b + 2\lambda/2$, $b + 3\lambda/2$ etc. where b denotes the distance of the point P from the transducer edge. Adding the contributions of all the Fresnel zones at point P (see Fig. 523 in [3]) we obtain, in a similar manner as before, the relation

$$z_r = z_{r1}/2. \tag{A2}$$

Hence it follows that the contribution of all the radiated waves in their extent outside of the transducer (embracing there all the Fresnel zones situated outside of the transducer), is equivalent to the contribution of one half of the first outside Fresnel zone z_{r1}.

If one assumes that the contribution (A2) will have the reverse phase than the contribution (A1) and remembering that the contributions of the Fresnel zones have the same amplitudes, then the contributions of the surface situated outside of the transducer disappear.

As a result, one obtains at the point P only the contributions of the transducer surface being a sum of the central wave (A1) and the edge wave (A2) with the reverse phase.

References

[1] M. Averkiou and M. Hamilton, *Nonlinear distortion of short pulses radiated by plane and focused circular pistons*, J. Acoust. Soc. Am., **102**, 2539–2547 (1997).

[2] L. Filipczyński, J. Wójcik, T. Kujawska, G. Łypacewicz, R. Tymkiewicz and B. Zienkiewicz, *Nonlinear native propagation effects of diagnostic ultrasound computed and measured in blood*, Ultrasound in Medicine and Biology, **27**, 2, 251–257 (2001).

[3] R. Grimsehl Tomaschek, Lehrbuch der Physik, Teubner, Berlin 1942, Vol. 1, pp. 387–388, Vol. 2, pp. 588–589.

[4] D. Hutchins and G. Hayward, *Radiated fields of ultrasonic transducers*, [in:] Physical Acoustics, vol. XIX, R. Thurston and A. Pierce [Eds.], Academic Press, Boston, London 1990, pp. 1–80.

[5] S. Kramer, S. McBride, H. Mair and D. Hutchins, *Characteristics of wide-band planar ultrasonic transducers using plane and edge wave contributions*, IEEE Transactions on Ultrasonics, Ferroelectrics and Frequency Control, **35**, 253–263 (1988).

[6] G. Łypacewicz and L. Filipczyński, *Measurement method and experimental study of ceramic transducer vibrations*, Acustica, **24**, 216–221 (1977).

[7] I. Malecki, *Physical foundations of technical acoustics*, Pergamon Press, Oxford and PWN, Warsaw 1969, p. 26.

[8] P. Morse and H. Feshbach, *Methods of theoretical physics*, McGraw Hill, New York 1953, pp. 495, 679.

[9] A. Petykiewicz, *Wave optics* [in Polish], Wydawnictwa Politechniki Warszawskiej, Warsaw 1980, pp. 121–126.

[10] R. Stephens and A. Bate, *Acoustics and vibrational physics*, Arnold Publishers, London 1966, p. 141.

[11] A. Rubinowicz, *Selected papers*, PWN, Warsaw 1975, pp. 462–463.

CHWILOWO ZAWIESZONE (bo patrz str 3 w.19-21 d)

These results were obtained numerically and confirmed experimentally. One should notice that the experimental pulse was a little longer than the numerical one due to small ringing effect at its end, however, the differences in the computed and measured spectra were very small.